Optical two-photon absorption in GaAs measured by optical-pump terahertz-probe spectroscopy

F. Kadlec,* H. Němec, and P. Kužel
Institute of Physics, Academy of Sciences of the Czech Republic, and Center for Molecular Systems and Biomolecules, Na Slovance 2, 182 21 Prague 8, Czech Republic

(Received 11 February 2004; revised manuscript received 7 May 2004; published 14 September 2004)

Time-resolved terahertz experiments in a novel setup were used for a direct observation of the competition between the single- and two-photon absorption in highly excited GaAs. The experiments were carried out near 800 nm where the single photon absorption usually dominates. The crystal surface was excited by femtosecond laser pulses with fluences up to 4.2 mJ/cm^2, for which the single-photon absorption saturates and the two-photon absorption becomes the leading absorption mechanism. The two-photon absorption coefficient β, its anisotropy and the depth profile of the photoexcited carriers were determined.

DOI: 10.1103/PhysRevB.70.125205 PACS number(s): 78.47.+p, 42.65.−k, 71.20.−b, 71.20.Nr

I. INTRODUCTION

Nonlinear properties of semiconductors remain an interesting and important topic in materials science. Among them, the two-photon absorption (TPA) is one of the most common mechanisms which provides a potentially powerful probe of high-energy conduction bands and yields information complementary to linear spectroscopies.[1] It also finds a variety of applications in optical communications, including optical switching[2] and ultrafast control of density of states in photonic crystals.[3] Recently, an interplay of single- and two-photon absorption has been investigated in order to coherently control photocurrent generation in bulk semiconductors.[4]

Usually, the TPA experiments are performed only with single photon energies below the linear absorption edge and there is a lack of experimental data for higher photon energies. To our knowledge there is only one work published in this field dealing with TPA in thin silicon films using photon energies above the indirect band gap.[5] On the other hand, due to the widespread use of femtosecond pulses from Ti:sapphire sources for the investigation of ultrafast carrier dynamics, the experiments often involve a considerable contribution of multiphoton processes. A detailed knowledge about the main absorption mechanisms at the relevant wavelengths is thus required, e.g., in order to estimate correctly the photoexcited carrier density.[6–8]

In this paper we present new experimental results concerning nonlinear absorption processes in GaAs obtained by means of optical-pump terahertz-probe (OPTP) experiments. The advantage of this technique compared to those using an optical probe is that the terahertz (THz) probe photons have energy in the meV range and cannot substantially modify the electronic distribution in the sample. Thus the THz radiation propagates practically without absorption and dispersion in unexcited bulk semi-insulating GaAs and can detect even low concentrations ($\approx 10^{14}$ cm^{-3}) of free carriers. On the other hand, highly excited parts of the sample behave like metallic mirrors reflecting the totality of the incident THz radiation. This property, which is a drawback when a classical transmission setup is used, allows us to conceive a time-of-flight THz technique. Thanks to the possibility of synchronous phase-sensitive detection of THz pulses one can sensitively monitor the position of the interface between the excited and unexcited part of the sample in a broad range of excitation fluences. The obtained experimental data then give access to the TPA coefficient.

II. EXPERIMENTAL

For our experiments we have used a Ti:sapphire multipass amplifier (Odin, Quantronix) delivering 1 mJ pulses with a duration of $\Delta t = 55$ fs, a bandwidth of $\Delta\lambda = 30$ nm, and a mean wavelength of $\lambda = 810$ nm at a repetition rate of 1 kHz. One part of the beam was used for the sample excitation; its intensity was varied by several orders of magnitude using neutral density filters. The sample was a $\langle 001 \rangle$ semi-insulating GaAs wafer with a thickness $d = 0.7$ mm fixed to a circular aperture with a diameter of 2 mm; the aperture was placed after the sample, so the beam excited a surface area (with a diameter of 5 mm) larger than that contributing to the signal. This setup should exclude the phenomena arising from a sharp step of the carrier density in the lateral direction. The in-plane orientation of the GaAs wafer was varied with regard to the pump beam polarization in order to study the anisotropy of the TPA. The THz radiation was generated and detected using 1 mm thick [011] ZnTe single crystals;[9] some more details about our THz setup were published previously.[10]

While usual OPTP studies[6,11,12] employ configurations where the THz beam transmissivity is detected, we have used a novel experimental scheme employing an internal reflection of the THz pulses. The propagation of pulses through the sample is shown schematically in Fig. 1. First, a THz pulse incident on the input surface is let to propagate through the sample in equilibrium. It is followed by the optical pump pulse, which generates free carriers near below the surface. The part of the THz pulse which passes through directly is not affected by the pump pulse and it is used as a reference. The part reflected on the output surface serves as a probe: It propagates back to the input surface, which has been excited meanwhile, and reflects from its inner side. Then, it can be detected as the first echo, carrying a signature of the excited input surface (and equilibrium output surface).

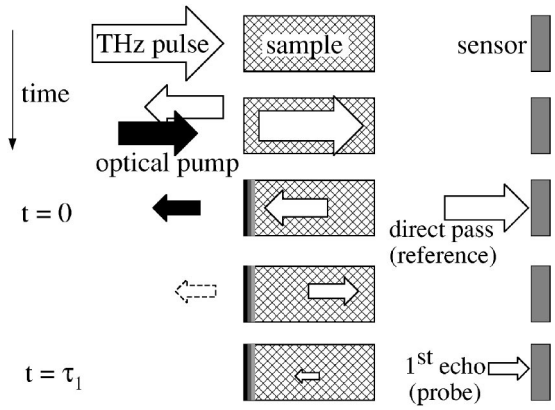

FIG. 1. The time sequence of pulses and their propagation through the sample (drawn out of scale). The area of arrows symbolizes the relative pulse energy.

The time of arrival of the first echo τ_1 provides information about the difference l between the path length of the directly passing THz pulse and that of the echo. In equilibrium (pump pulse off), the reflection occurs on the crystal surface so that $l=2d$. At low excitation fluences the pump pulse is absorbed by SPA within the penetration depth $\Delta=1/\alpha_0=0.75$ μm (where α_0 is the linear absorption coefficient in GaAs at 800 nm)[13] and the effective path of the 1st echo will be slightly shortened. At higher fluences, the photoexcited layer at the sample surface becomes optically bleached and its thickness may increase. On the other hand, at high fluences the nonvanishing TPA reduces the total number of particles excited through SPA. The photoexcited layer thickness will thus depend on the competition between TPA and saturated SPA.

The probe THz pulse is reflected on the interface separating the sample in equilibrium from the photoexcited region, which has a metallike character and is opaque in the THz range. For simplicity, we assume for a while that the change of optical constants at the interface is steplike. Then, $l=2(d-z_0)$, where z_0 is the interface distance from the sample input face. The temporal advance of the echo with respect to that obtained without pump pulse is equal to $\tau=2n_{\mathrm{THz}}z_0/c$, where $n_{\mathrm{THz}}=3.55$ is the refractive index of unexcited GaAs at THz frequencies. Experimentally, the excited layer thickness z_0 was measured as a function of the pump pulse fluence up to $\Phi_0=4.2$ mJ/cm^2.

III. THEORETICAL DESCRIPTION

To describe the competition of the TPA and saturated SPA processes quantitatively, we assume that the TPA is the only effective process based on the nonlinear third-order susceptibility $\chi^{(3)}_{ijkl}$, i.e., we neglect the possible self-phase modulation and self-focusing of the pump laser beam. The TPA is expected to be anisotropic due to the tensorial properties of the nonlinear susceptibility which has three independent coefficients for GaAs in the degenerate TPA case, namely $\chi^{(3)}_{1111}$, $\chi^{(3)}_{1122}$, and $\chi^{(3)}_{1221}$.[14,15] One can easily find for the pump beam propagation along $\langle 001\rangle$

$$\beta=\beta_{[100]}\cos^2 2\theta+\beta_{[110]}\sin^2 2\theta, \tag{1}$$

where $\beta_{[100]}\propto \mathrm{Im}\,\chi^{(3)}_{1111}$ and $\beta_{[110]}\propto \mathrm{Im}(\chi^{(3)}_{1111}+\chi^{(3)}_{1122}+2\chi^{(3)}_{1221})/2$ are the two independent TPA coefficients and where θ is the angle between the crystallographic direction $\langle 100\rangle$ and the pump polarization.

The pump beam size is larger than the probed area, hence we assume additionally that the pump beam is homogeneous in the lateral plane. Moreover, for sub-100 fs pulses at 810 nm the free-carrier absorption can be neglected.[16,17] The propagation of the optical pump pulse in the direction perpendicular to the surface of GaAs ($\parallel z$-axis) is then described by the following pair of differential equations

$$\frac{\partial I(z,t)}{\partial z}=-\alpha(n)I(z,t)-\beta I^2(z,t)-\frac{1}{v_g}\frac{\partial I(z,t)}{\partial t}, \tag{2}$$

$$\frac{\partial n(z,t)}{\partial t}=\frac{\alpha(n)}{\hbar\omega}I(z,t). \tag{3}$$

where $I(z,t)$ is the pump beam intensity, $n(z,t)$ is the density of SPA-excited particles (electrons in the conduction band or holes in the valence band), ω is the angular frequency of the pump pulse, and v_g is its group velocity in GaAs. As the optical pump pulse lasts for several tens of femtoseconds only, no significant relaxation or redistribution of $n(z,t)$ can occur during the excitation process (see Sec. IV). The SPA coefficient α is assumed to depend on n, i.e., $\alpha=\alpha(n(z,t))$ owing to the band filling. It should be proportional to the density of available states

$$\alpha(n)=\alpha_0\frac{n_{\max}-n}{n_{\max}}, \tag{4}$$

where $n_{\max}$ is the population inversion threshold. Using (4), Eq. (3) can be integrated in time. Denoting $\Phi(z)=\int_{-\infty}^{\infty}I(z,t)dt$ the pump fluence coming through a thin layer of sample at the depth z, and $n_{\mathrm{SPA}}(z)=n(z,t\to\infty)$ the total density of SPA-excited electrons at z, one finds

$$n_{\mathrm{SPA}}(z)=n_{\max}(1-e^{-\Phi(z)/\Phi_s}), \tag{5}$$

where Φ_s is the saturation fluence defined by

$$\Phi_s\alpha_0=\hbar\omega n_{\max}. \tag{6}$$

The saturation behavior described by Eq. (5) will be denoted as Model I. We will also discuss a simple and useful approximation of Eq. (5) (denoted as Model II)

$$\Phi\leqslant\Phi_s:\ n_{\mathrm{SPA}}(z)=n_{\max}\,\Phi(z)/\Phi_s,$$

$$\Phi>\Phi_s:\ n_{\mathrm{SPA}}(z)=n_{\max}. \tag{7}$$

Both models are shown in the inset of Fig. 2. Let us neglect the possible reshaping of the pump pulse due to nonlinearities; in this case the intensity $I(z,t)$ can be factorized

$$I(z,t)=\Phi(z)i_0(z-v_gt). \tag{8}$$

Substituting (8) and (3) into Eq. (2) and integrating it over t one obtains

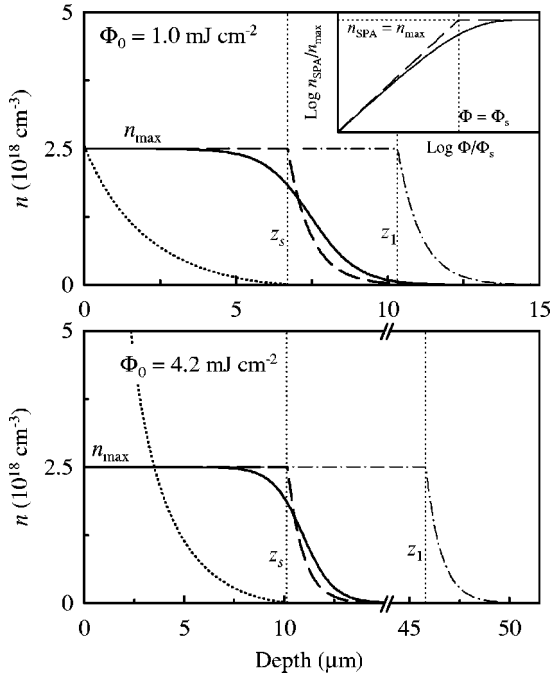

FIG. 2. Density of free carriers generated by TPA and SPA near the surface of the sample for two incident pump fluences Φ_0; parameters: $\beta' = 1.1 \times 10^{23}$ J^{-2} m, $n_{max} = 2.5 \times 10^{18}$ cm^{-3}. Model I: n_{SPA} (solid line), n_{TPA} (dotted line); Model II: n_{SPA} (dashed line), hypothetical n_{SPA} for $\beta' = 0$, i.e., neglecting the TPA (dash-dotted line). Inset: Density of SPA-carriers versus the light fluence; Model I (solid line), Model II (dashed line).

$$\frac{d\Phi(z)}{dz} = -\hbar\omega n_{SPA}(z) - \beta\Phi^2(z)\rho/\Delta t, \tag{9}$$

where ρ is a numerical factor which depends on the pulse shape (e.g., $\rho = 1$ for a rectangular pulse, $\rho = 0.67$ for a Gaussian pulse). The meaning of this factor can be slightly extended: Its value may additionally account for the pump pulse reshaping due to nonlinear interactions. For this reason, even if the pulse shape is exactly known, the effective value of ρ can exhibit some uncertainty. Equation (9) along with (5) or (7)—Models I or II, respectively—are the starting points of our analysis of the experimental results. We have a direct experimental access to the z-position of the drop-down of n_{SPA} which is rather sharp (sub-1 μm). The fitting of this position to the solution of (9) then provides the parameters n_{max} and

$$\beta' = \frac{\beta\rho}{\hbar\omega\Delta t}. \tag{10}$$

Both these quantities can be relatively precisely obtained from our experiment. The complete spatial profile of $n_{SPA}(z)$ and that of the carriers excited through the TPA process

$$n_{TPA}(z) = \beta'\Phi(z)^2/2 \tag{11}$$

then can be determined.

The solution of Eq. (9) can be found numerically for both saturation models. Moreover, an approximate analytical solution giving a better insight into the problem can be also easily obtained assuming that the TPA process is significant only in a thin slab near the surface where the SPA is saturated. This means that Eq. (9) exhibits two different regimes: (i) in a thin layer close to the surface, $n_{SPA} \simeq n_{max}$ with an arbitrarily high n_{TPA} and (ii) deeper in the sample, $n_{SPA} < n_{max}$ while $n_{TPA} \ll n_{SPA}$. This is accounted for by the following condition:

$$\frac{\beta'}{n_{max}}\Phi_s^2 \ll 1. \tag{12}$$

which, as we show later, is satisfied in GaAs for our experimental conditions.

An approximate solution of (9) for Model I then reads (see Appendix for details):

$$\Phi(z) = \Phi_s \ln\{1 + [e^{\Phi_i/\Phi_s} - 1]e^{-\alpha_0(z - z_s + z_1)}\}, \tag{13}$$

where

$$z_1 = \frac{1}{\alpha_0}\left(\frac{\Phi_i}{\Phi_s} - 1\right), \tag{14}$$

$$z_s = \frac{1}{\hbar\omega\sqrt{n_{max}\beta'}} \arctan\left[\frac{(\Phi_i - \Phi_s)\sqrt{\beta'/n_{max}}}{1 + \Phi_i\Phi_s\beta'/n_{max}}\right], \tag{15}$$

and where $\Phi_i = (1-R)\Phi_0$ is the incident pump fluence (corrected by the Fresnel losses R due to the reflection on the input surface). Note that the photoinduced change of the optical reflectivity is smaller than 1% for our experimental conditions.[18–20] The physical meaning of the parameters z_s and z_1 becomes clear from Fig. 2 which is plotted for a model set of parameters and for two incident fluences. For incident fluences Φ_i exceeding the saturation fluence Φ_s, there is a layer near the surface where the concentration of SPA-excited electrons is approximately equal to n_{max}. The position z_s is of our fundamental interest: It defines the depth where the concentration of SPA-excited particles start to decay rapidly. On the other hand, the position z_1 can be identified with a rapid drop-down of the concentration of SPA-excited particles in a hypothetical model with vanishing TPA. For low fluences, these positions practically coincide and the slope of their dependence on Φ_i provides information on n_{max}. For higher fluences, the curve $z_s(\Phi_i)$ saturates due to TPA and the saturation value provides the parameter β'.

IV. RESULTS AND DISCUSSION

We excite with an excess energy of 125 meV above the band-gap. Taking into account the interband transitions both from the heavy-hole and from the light-hole valence bands and the bandwidth of the pump pulses, we can estimate the density of states in the conduction band which can be filled by electrons through SPA. However, this quantity depends to some extent on the degree of redistribution of the free carriers in the energy space during the excitation process which lasts about 55 fs. Two limiting cases can be considered.

(i) One assumes that no significant relaxation or redistribution of the photoexcited electron density in the energy space occurs so fast. Then, within the spectral full-width-at-

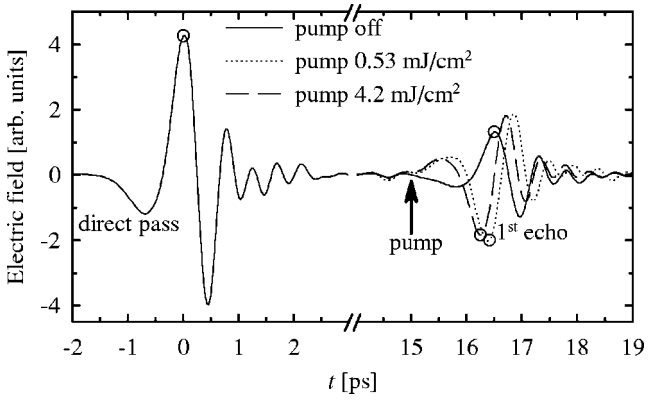

FIG. 3. Measured waveforms of the transmitted THz field. Small circles indicate equivalent points on the reference and signal echoes.

half-maximum (FWHM) of the pump pulse, free electrons can be created with 50–150 meV excess energy above the bottom of the conduction band. It leads to the density of available states of 4×10^{18} cm^{-3}.

(ii) One assumes a very fast and efficient redistribution of electrons during 55 fs. Then all the states between the bottom of the conduction band and the excess energy of about 180 meV (corresponding to twice the FWHM of the pump pulse) may become available: this corresponds to the density of 6×10^{18} cm^{-3}.

Clearly, neither of these limits is realistic and the true experimental value should lie in between. The electron-LO phonon interaction occurs usually on the timescale of hundreds of femtosecond and will not significantly contribute to the energy redistribution during the pump pulse duration.[21] The carrier-carrier scattering process may be efficient on shorter time scales. On the other hand, it has been shown[22] that this last process is limited at high carrier densities owing to the Pauli blocking of the states at the bottom of the conduction band and owing to an efficient femtosecond buildup of screening of the Coulomb interaction.

Thus, it seems reasonable to expect the critical bleaching concentration of free electrons (and holes) corresponding to the population inversion threshold (one half of the available states) to be $n_{\max}=2.5\times10^{18}$ cm^{-3} with an error smaller than 0.5×10^{18} cm^{-3}.

For $\Phi_0\gtrsim70$ μJ/cm^2 the measured waveforms are very similar to that represented by the dotted line in Fig. 3. The phase of the first echo is changed by π owing to the reflection on the conductive photoexcited layer (optically denser medium) but its temporal shape matches well that of the direct pass. Note that the integrated power of this echo is higher than in equilibrium, because the reflection coefficient on a metallike surface is close to unity.

For $\Phi_0=70$ μJ/cm^2 the concentration of carriers at the surface is just equal to $n_{\max}$ and the experimentally obtained advance of the echo is equal to $\tau=20\pm12$ fs. This corresponds to the excited layer thickness of 0.85 ± 0.5 μm which is in agreement with the expected linear penetration depth of 0.75 μm in GaAs. All these findings mean that we may define an effective position of the interface where the THz echo is reflected as

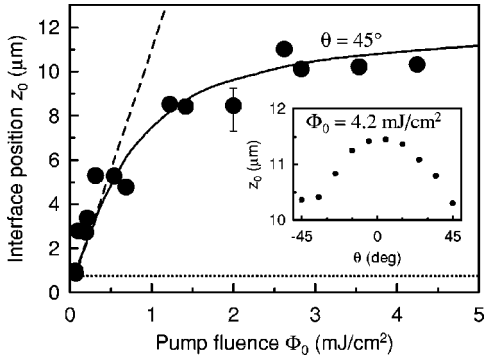

FIG. 4. Interface position versus incident pump fluence (pump polarization$\|$[110]). Points: experimental data; solid line: fit using Eqs. (16) and (15); dotted line: linear penetration depth $1/\alpha_0$; dashed line: Hypothetical interface position for vanishing TPA ($\beta=0$). Inset: Angular dependence of the interface position for $\Phi_0=4.2$ mJ/cm^2.

$$z_0 = z_s + 1/\alpha_0, \tag{16}$$

and that, within the experimental uncertainty, both models described in the previous section may be equivalently used for the description of the experiment. We have verified for a large number of incident fluences that the shape of the 1st THz echo does not differ significantly from that of the reference one and we have measured the temporal advance τ of these echoes compared to the equilibrium situation; subsequently, we have deduced the interface position z_0 and the saturation depth z_s.

For high fluences we have found a significant anisotropy of z_0 which depends on the pump beam polarization. Figure 4 shows the experimental results. Fitting the results using formula (15) confirms the predicted value of the saturated concentration $n_{\max}$ and provides the value of the nonlinear coefficients $\beta'_{[110]}=1.1\times10^{23}$ J^{-2} m and $\beta'_{[100]}=0.9\times10^{23}$ J^{-2} m which allows us to estimate the TPA coefficients: $\beta_{[110]}=220\pm50$ cm/GW and $\beta_{[100]}=180\pm50$ cm/GW using the Gaussian approximation of the temporal pulse shape. The uncertainty in the absolute values of the TPA coefficients β is rather large because the shape of the incident pulse and, consequently, the value of ρ, are not precisely known. On the other hand, the anisotropy of the TPA coefficient $(2\,\mathrm{Im}\,\chi^{(3)}_{1221}+\mathrm{Im}\,\chi^{(3)}_{1122})/\mathrm{Im}\,\chi^{(3)}_{1111}=1.45$ is quite accurate. This result is close to the values 1.4 ± 0.3 and 1.76 ± 0.08 obtained earlier at 1064 nm[23] and at 950 nm,[15] respectively.

Note that we have used the results of our fit to plot the curves in Fig. 2; thus, they provide a true picture of the carrier distribution at the surface of GaAs upon high-intensity photoexcitation with fs pulses. In a thin layer close to the surface the density of carriers excited through the TPA process largely exceeds $n_{\max}$: For the largest used excitation fluence one obtains $n_{\mathrm{TPA}}=3.7\times10^{19}$ cm^{-3} and 4.4×10^{19} cm^{-3} at the surface for the [100] and [110] polarization directions, respectively. On the other hand, $n_{\mathrm{TPA}}(z)$ rapidly decreases and, depending on the input fluence, it becomes negligible within 4–7 μm depth. The left-hand side

of the inequality (12) reaches 0.01 which validates our analytical solution.

The experimental values of β found in the literature[15,16,24] span over the range of 20–30 cm/GW for excitation wavelengths well below the band gap (1064 and 950 nm). In the theory Im $\chi^{(3)}$ is proportional to the sum of two-photon momentum matrix elements over all the states in the valence and conduction bands [with energies $E_v(k)$ and $E_c(k)$, respectively] which satisfy the energy conservation law expressed by the presence of a Fermi Golden rule delta function $\delta(E_c(k)-E_v(k)-2\hbar\omega)$.[25–28] As all the relevant momentum matrix elements are nonresonant, they are not expected to exhibit a large dispersion. In a rough approximation, the main dispersion is assumed to arise from the summation over the delta function which can be converted to the joint density of states for the valence and conduction bands. At the same time, the joint density of states determines also to a large extent the behavior of the imaginary part of the linear permittivity ($\epsilon=\epsilon_1+i\epsilon_2$).[29] We can thus write within a first semiquantitative approximation (cf. Ref. 27):

$$\beta(\omega) \propto \omega \frac{\epsilon_2(2\omega)}{\epsilon_1(2\omega)}. \tag{17}$$

Using the data for the dispersion of ϵ in GaAs[30] and Eq. (17) one can estimate the expected ratio $\beta(800\text{ nm})/\beta(1064\text{ nm}) \approx 9$ and $\beta(800\text{ nm})/\beta(950\text{ nm}) \approx 5$. This indicates that with decreasing photon wavelength, the TPA coefficient is expected to exhibit a strong enhancement and to reach values exceeding 100 cm/GW. We believe that this enhancement is unambiguously observed in our experiments and we interpret it as due to resonant two-photon transitions into the *L*-valley.

V. CONCLUSION

We have introduced a new experimental scheme of THz probing of photoexcited semiconductors and we have demonstrated its usefulness by determining the two-photon absorption coefficient of GaAs at 800 nm and its anisotropy. To our knowledge, we have performed the first experimental evaluation of β in the spectral range exceeding the direct gap energy. The underlying model allows us to quantify the competition between the single- and two-photon absorption and to calculate the photoexcited carrier densities as a function of the distance from the sample surface. Finally, our experiments identify an upper limit for the photoexcited electron density in GaAs using pump photons with low excess energy (typically Ti:sapphire lasers), which has been often overestimated in previous works.

ACKNOWLEDGMENTS

We would like to thank J.-F. Roux and J. Oswald for helpful comments. The financial support of the Ministry of Education of the Czech Republic (project No. LN00A032) is acknowledged.

APPENDIX: SOLUTION OF THE MODELS

In this Appendix we solve Eq. (9) assuming approximation (12). The description by means of model I is probably more realistic, however, we start the analysis with model II, which provides a clear insight into the solution.

Close to the sample surface $n_{\mathrm{SPA}}=n_{\max}$, Eq. (9) then becomes:

$$\frac{1}{\hbar\omega}\frac{d\Phi(z)}{dz} = -n_{\max} - \beta'\Phi^2(z). \tag{A1}$$

One finds after the integration

$$\Phi(z) = \Phi_i \frac{1 - X(z)/U}{1 + UX(z)}, \tag{A2}$$

where

$$U = \Phi_i \sqrt{\frac{\beta'}{n_{\max}}},$$

$$X(z) = \tan(\hbar\omega\sqrt{n_{\max}\beta'}z).$$

Equation (A2) describes how the pump radiation fluence is depleted due to the TPA and due to the saturated SPA from the initial value Φ_i at the surface down to Φ_s at the so called saturation depth z_s defined by $\Phi(z_s)=\Phi_s$. Using (A2), this leads to Eq. (15) for z_s.

Following the condition (12), TPA is negligible at z_s. Thus for $z>z_s$ Eq. (9) yields a linear absorption process

$$\Phi(z) = \Phi_s e^{-\alpha_0(z-z_s)}. \tag{A3}$$

In the case of a weak TPA ($\beta' \to 0$) the profile of the carrier density is the same but one obtains a modified saturation depth z_1

$$z_s \to z_1 = \frac{1}{\alpha_0}\left(\frac{\Phi_i}{\Phi_s} - 1\right). \tag{A4}$$

Physically it means that, in the region where SPA is saturated, the TPA process depletes a number of photons, which depends on Φ_i and β'. This number directly determines the position of the interface between the excited and unexcited region but it does not influence its shape.

Concerning model I, let us start the analysis by the case of negligible TPA ($\beta'=0$). Then the equation

$$\frac{1}{\hbar\omega}\frac{d\Phi(z)}{dz} = -n_{\max}[1 - e^{-\Phi(z)/\Phi_s}], \tag{A5}$$

has to be solved. One finds after integration

$$\Phi(z) = \Phi_s \ln\{1 + [e^{\Phi_i/\Phi_s} - 1]e^{-\alpha_0 z}\}. \tag{A6}$$

The drop-down in the carrier density n_{SPA} is then found near $z=z_1$. Taking into account the arguments given above, in the case of a nonvanishing β' the drop-down of n_{SPA} occurs at z_s in a very good approximation. This can be accounted for by a linear transformation of coordinates: $z \to z - z_s + z_1$ which leads to the formula (13) for the fluence and to the following profile of n_{SPA} (see Fig. 2)

$$n_{\mathrm{SPA}}(z) = n_{\max}\left\{1 - \frac{1}{1 + [e^{\Phi_i/\Phi_s} - 1]e^{-\alpha_0(z-z_s+z_1)}}\right\}. \tag{A7}$$

We have verified by a numerical calculation that this equa-

tion is an excellent approximation of the exact solution. The difference of the interface positions provided by Eq. (A7) and by a numerical solution of Eq. (9) is smaller than 50 nm for our experimental conditions.

*Electronic address: kadlecf@fzu.cz

[1] R. W. Boyd, *Nonlinear Optics* (Academic, San Diego, 1992).
[2] F. Lacassie, D. Kaplan, T. D. Saxce, and P. Pignolet, Eur. Phys. J. A **11**, 189 (2000).
[3] P. M. Johnson, A. F. Koenderink, and W. L. Vos, Phys. Rev. B **66**, 081102(R) (2002).
[4] J. M. Fraser and H. M. van Driel, Phys. Rev. B **68**, 085208 (2003).
[5] D. H. Reitze, T. R. Zhang, W. M. Wood, and M. C. Downer, J. Opt. Soc. Am. B **7**, 84 (1990).
[6] G. Segschneider, F. Jacob, T. Löffler, H. G. Roskos, S. Tautz, P. Kiesel, and G. Döhler, Phys. Rev. B **65**, 125205 (2002).
[7] T. S. Sosnowski, T. B. Norris, H. H. Wang, P. Grenier, J. F. Whitaker, and C. Y. Sung, Appl. Phys. Lett. **70**, 3245 (1997).
[8] U. Siegner, R. Fluck, G. Zhang, and U. Keller, Appl. Phys. Lett. **69**, 2566 (1996).
[9] A. Nahata, A. S. Weling, and T. F. Heinz, Appl. Phys. Lett. **69**, 2321 (1996).
[10] P. Kužel and J. Petzelt, Ferroelectrics **239**, 949 (2000).
[11] A. Leitenstorfer, C. Fürst, A. Laubereau, and W. Kaiser, Phys. Rev. Lett. **76**, 1545 (1996).
[12] M. Beard, G. Turner, and C. Schmuttenmaer, Phys. Rev. B **62**, 15764 (2000).
[13] *Handbook of the Optical Constants of Solids*, edited by E. Palik (Academic Press, New York, 1985).
[14] G. S. He and S. H. Liu, *Physics of Nonlinear Optics* (World Scientific, Singapore, 1999).
[15] M. D. Dvorak, W. A. Schroeder, D. R. Andersen, A. L Smirl, and B. S. Wherrett, IEEE J. Quantum Electron. **30**, 256 (1994).
[16] J. H. Bechtel and W. L. Smith, Phys. Rev. B **13**, 3515 (1976).
[17] W. G. Spitzer and J. M. Whelan, Phys. Rev. **114**, 59 (1959).
[18] J.-F. Roux, J.-L. Coutaz, and A. Krotkus, Appl. Phys. Lett. **74**, 2462 (1999).
[19] F. Ganikhanov, K. Burr, D. Hilton, and C. L. Tang, Phys. Rev. B **60**, 8890 (1999).
[20] J. P. Callan, A. M.-T. Kim, L. Huang, and E. Mazur, Chem. Phys. **251**, 167 (2000).
[21] J. Shah, *Ultrafast Spectroscopy of Semiconductors and Semiconductor Nanostructures* (Springer-Verlag, Heidelberg, 1996).
[22] F. Camescasse, A. Alexandrou, and D. Hulin, Phys. Status Solidi B **204**, 293 (1997).
[23] S. J. Bepko, Phys. Rev. B **12**, 669 (1975).
[24] G. C. Valley and T. F. Bogges, J. Appl. Phys. **66**, 2407 (1989).
[25] D. C. Hutchings and B. S. Wherrett, Phys. Rev. B **49**, 2418 (1994).
[26] M. Murayama and T. Nakayama, Phys. Rev. B **49**, 5737 (1994).
[27] M. Murayama and T. Nakayama, Phys. Rev. B **52**, 4986 (1995).
[28] M. Murayama and T. Nakayama, Phys. Rev. B **55**, 9628 (1997).
[29] P. Y. Yu and M. Cardona, *Fundamentals of Semiconductors* (Springer-Verlag, Berlin Heidelberg, 1996).
[30] D. Aspnes and A. Studna, Phys. Rev. B **27**, 985 (1983).